PAPER Special Issue on Spread Spectrum Techniques and Applications

Spread Spectrum Pulse Position Modulation ——A Simple Approach for Shannon's Limit——

Isao OKAZAKI†* and Takaaki HASEGAWA†, *Members*

SUMMARY In this paper, we propose a spread spectrum pulse position modulation (SS-PPM) system, and describe its basic performances. In direct sequence spread spectrum (DS/SS) systems, pseudo-noise (PN) matched filters are often used as information demodulation devices. In the PN matched filter demodulation systems, for simple structure and low cost of each receiver, it is desired that each demodulator uses only one PN matched filter, and that signals transmitted from each transmitter are binary. In such systems, on-off keying (SS-OOK), binary-phase-shift keying (SS-BPSK) and differential phase-shift keying (SS-DPSK) have been conventionally used. As one of such systems, we propose the SS-PPM system; the SS-PPM system is divided into the following two systems: 1) the SS-PPM system without sequence inversion keying (SIK) of the spreading code (Without SIK for short); 2) the SS-PPM system with SIK of the spreading code (With SIK for short). As a result, we show that under the same bandwidth and the same code length, the data transmission rate of the SS-PPM system is superior to that of the other conventional SS systems, and that under the same bandwidth, the same code length and the same data transmission rate, the SS-PPM system is superior to the other conventional SS systems on the following points: 1) Single channel bit error rate (BER) (BER characteristics of the SS-PPM system improve with increasing the number of chip slots of the SS-PPM system, and as the number of chip slots increases, it approaches Shannon's limit); 2) Asynchronous CDMA BER; 3) Frequency utilization efficiency. In addition, we also show that With SIK is superior to Without SIK on these points.

key words: *spread spectrum, PPM, DPPM, code-division multiple access, matched filter*

1. Introduction

In direct sequence spread spectrum (DS/SS) systems, pseudo-noise (PN) matched filters are often used as information demodulation devices because of the following advantages: 1) Essentially making PN code acquisition and tracking unnecessary; 2) Simple structure and low cost of each receiver; 3) Making small-sized and lightweight receiver possible. In the PN matched filter demodulation systems, for simpler structure and lower cost of each receiver, it is desired that each demodulator uses only one PN matched filter, and that signals transmitted from each transmitter are binary.

Manuscript received January 13, 1993.
Manuscript revised April 3, 1993.

† The authors are with the Faculty of Engineering, Saitama University, Urawa-shi, 338 Japan.
* Presently, with NTT Radio Communication Systems Laboratories, Yokosuka-shi, 238-03 Japan.

In such systems, two conventional systems have been widely used. One is an on-off keying (SS-OOK) system [1, etc.]; 1 or 0 of input information data corresponds to on or off of the SS signals (PN codes or spreading codes). The other is a binary-phase-shift keying (SS-BPSK) system or a differential phase-shift keying (SS-DPSK) one [2, etc.]; input information data correspond to phase 0 or π of the SS signal's carrier waves. Therefore, when one data bit is transmitted every spreading code period, the data transmission rate is to be maximum ($1/T$ [bit/sec] when a period of the spreading code is T [sec]) in these systems.

In addition to these binary output systems, to increase the data transmission rate, we propose a spread spectrum pulse position modulation (SS-PPM) system [6]-[13]. The SS-PPM system uses the orthogonality of the SS signal shifted with more than one chip interval, and transmits information as the position of the SS signal similar to a digital pulse position modulation (DPPM) system; namely, in this system, input information data correspond to the position of the SS signal shifted with more than one chip interval. The SS-PPM system is divided into the following two systems [10]-[13]: 1) The SS-PPM system without sequence inversion keying (SIK) of the spreading code (Without SIK for short); 2) The SS-PPM system with SIK of the spreading code (With SIK for short).

As a result, we will show that the SS-PPM system is superior to the SS-OOK, the SS-BPSK or the SS-DPSK one, and that With SIK is superior to Without SIK on the following points: 1) Data transmission rate [6], [8], [10]-[13]; 2) Single channel BER [6]-[8], [10]-[13]; 3) Asynchronous CDMA BER [9]-[13]; 4) Frequency utilization efficiency.

As a system that input information data correspond to the position of the SS signal shifted with more than one chip interval, another approach has already been reported [3]. However it is not a binary output system, and its signal structure is different from the SS-PPM system's one. On the other hand, in the time spread system, time spread pulse position modulation (TS-PPM) was reported [4], [5] after we reported the SS-PPM system.

The purpose of this work is to make clear the performance of the SS-PPM system.

2. Principles of SS-PPM [6]-[13]

In this section, we describe the principles of the SS-PPM system. Firstly, we show a signal structure of the SS-PPM system. Secondly, we illustrate a basic structure of the SS-PPM system. Table 1 shows the notations on the following discussions.

2. 1 Signal Structure of SS-PPM [6]-[13]

Figure 1 shows a signal structure of the SS-PPM system (horizontal axis represents time). Since the PN signal exists partially in a frame, the envelope is discontinuous as shown in Fig. 1. The SS-PPM system has a frame; the frame consists of $(M+L-1)$ slots. In each frame, there exists one spreading code, and its code length is L [chip]. The duration of one slot equals to one chip duration of the spreading code.

This system transmits information as the position of the spreading code similar to the DPPM system. In the first part of the frame, a spreading code starts from a certain slot out of M slots, and continues for L chips from the start slot. Thus, the first chip of the spreading code can locate in one of M slots from the first slot to the M-th slot in each frame. The front part allocated M slots is termed information slots. On the other hand, in the latter part of the frame, to prevent the neighboring frame's spreading codes from overlapping, there locate $(L-1)$ slots as guard zone. Thus, the SS-PPM system is one of the binary output systems (signals transmitted from each transmitter are binary) [6]-[13].

Therefore, the SS-PPM system without sequence inversion keying (SIK) of the spreading code (Without SIK for short) can transmit $\log_2 M$ [bit/frame], and it corresponds to M-ary orthogonal modulation systems [11]-[12]. On the other hand, the SS-PPM system with SIK of the spreading code (With SIK for short) can transmit $\log_2 2M$ [bit/frame], and it corresponds to 2M-ary bi-orthogonal modulation systems [11].

Moreover, since the SS-PPM system substantially has the advantage of the DPPM system, this system is expected to have low power transmission capability using a long frame. On the other hand, the SS-PPM system, unlike the DPPM system, has the ability of asynchronous CDMA using many spreading codes.

Table 1 Notations.

Number of Information Slots per Frame	M [slot]
Length of Spreading Code (= Length of PN Code or Number of Step of PN Matched Filter)	L [chip]
Chip Rate of Spreading Code	R_c [cps]
Number of Multiplex Channels	m [channel]

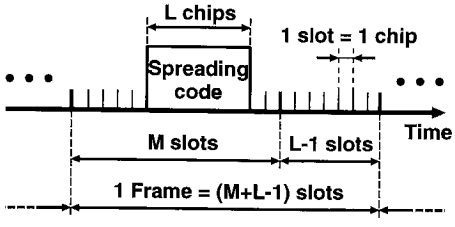

Fig. 1 Signal structure of the SS-PPM system.

2. 2 System Structure of SS-PPM [8], [10]-[13]

Figure 2 shows a basic structure of the SS-PPM system (Without SIK). This system is an example of coherent detection systems, but the SS-PPM system can also perform as an envelope detection system or a baseband one of course.

The transmitter of the SS-PPM acts as follows.

First, input data, which come into the transmitter, are converted into $\log_2 M$ bit data for making up a frame of DPPM (serial parallel conversion); the DPPM pulse is used as a trigger, and an L-chip-length spreading code is generated (it is a SS-PPM signal). After that, the carrier wave of frequency f_c [Hz] is modulated by this SS-PPM signal, and transmitted.

The receiver of the SS-PPM system acts as follows.

The received carrier band signal is detected coherently, and obtains the SS-PPM signal. After that, the SS-PPM signal comes into the PN matched filter; at the input of the PN matched filter, a soft decision is carried out. If the input spreading code matches the pattern of the PN matched filter, one chip length sharp pulse is produced at the position corresponding to the transmitted data. It depends on the orthogonality of the spreading code shifted with more than one chip. Thus output data is decided by the position of this pulse.

In the next section, we evaluate the performance of the SS-PPM system.

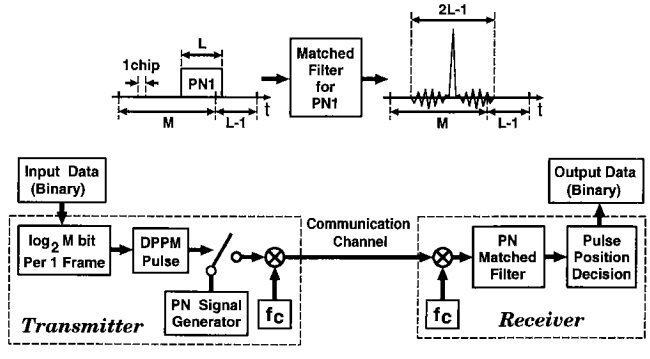

Fig. 2 Structure of a SS-PPM system.

3. Data Transmission Rates Properties [6], [8], [10] -[13]

From the discussion of Sect. 2. 1, the data transmission rate of the single channel SS-PPM system expresses as the following two equations [8], [10]-[13]:

- Without SIK:

$$R_{Without}=\frac{(\log_2 M)R_c}{M+L-1}\ [\text{bit/sec}] \tag{1}$$

- With SIK:

$$R_{With}=\frac{(\log_2 2M)R_c}{M+L-1}\ [\text{bit/sec}] \tag{2}$$

where, M is the number of information slots, L is the length of spreading code and R_c is the chip rate of the spreading code as shown in Table 1.

From these equations, we calculate and show the data transmission rates. Figure 3 illustrates the data transmission rates of single channel Without SIK versus the number of information slots M for various length of spreading code (L=63, 127, 255, 511 and 1023 [chip]). Figure 4 illustrates the data transmission rates of single channel With SIK versus the number of information slots M for various length of spreading code (L=63, 127, 255, 511 and 1023 [chip]). Though the values of data transmission rates are discrete (M= 2, 4, 8, 16, ··· [slot]) in these figures, plots are connected to guide the reader's eye by a dashed line for each L in these figures. The chip rate of the spreading code R_c is 12.7×10^6 [cps] ([chip/second]). In addition, we also illustrate the maximum data transmission rate of the SS-OOK, the SS-BPSK or the SS-DPSK system, which uses just one PN matched filter and binary baseband signals, as the solid line. Their chip rate of the spreading code is the same as the SS-PPM system's one, and their length of the spreading code L is 127 [chip]; namely their data transmission rate is 100 [Kbps] ([Kilo bit/sec]).

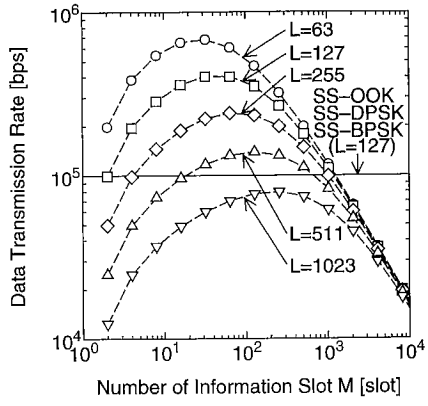

Fig. 3 Data transmission rates of single channel Without SIK for various L ($R_c=12.7\times10^6$ [cps]).

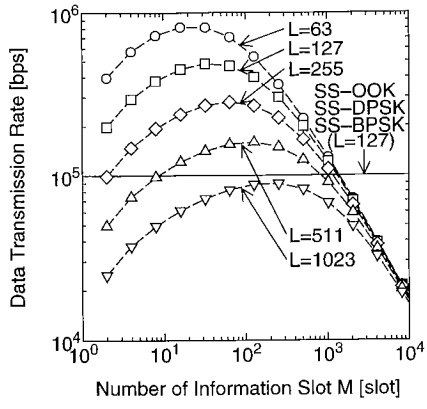

Fig. 4 Data transmission rates of single channel With SIK for various L ($R_c=12.7\times10^6$ [cps]).

These figures show that under the same L, the data transmission rate of the SS-PPM system is greater than that of the other conventional SS systems in some range of M. At L=127 [chip], for example, the maximum data transmission rate of the SS-PPM system is 4.0 times (Without SIK) or 4.8 times (With SIK) higher than those of the other conventional SS systems [10]-[13]. Furthermore, the maximum data transmission rate of With SIK is higher than that of Without SIK at the same L. At L=127 [chip], for example, the maximum data transmission rate of With SIK is 1.2 times higher than that of Without SIK [10], [11], [13].

Moreover, Table 2 shows the values of M of Without SIK and of With SIK at the same data transmission rate on condition that m is 1 [channel], and L is 127 [chip], and R_c is 12.7×10^6 [cps]. This table shows that the values of M of With SIK are larger than those of M of Without SIK one at the same data transmission rate [11], [13].

As mentioned above, the structure of the SS-PPM system's receiver is simple because the receiver uses only one PN matched filter, and signals transmitted from each transmitter are binary, in addition the maximum data transmissiom rate of the SS-PPM system is higher than that of the SS-OOK, the SS-BPSK or the SS-DPSK system under the same bandwidth and the same length of spreading code. The maximum data transmission rate of With SIK is higher than that of

Table 2 The values of M of Without SIK and of With SIK at the same data transmission rate (m=1 [channel], L=127 [chip], $R_c=12.7\times10^6$ [cps]).

Data Transmission Rate [Kbps]	M [slot/frame] of Without SIK	M [slot/frame] of With SIK
402	32	126
401	64	127
350	128	183
266	256	319
179	512	599
110	1024	1160
100	1168	1317

Table 3 Conditions of computer simulation and theoretical analysis.

Spreading Code	M Sequences
Detection	Coherent Detection
Decision	Decision of Maximum Likelihood from Each Slot's Correlation
Additive Noise	White Gaussian Noise (WGN)
Synchronization of the Frame in Each Channel	Not Considered
Chip Synchronization among Multiplex Channels	Not Carried Out (Asynchronous CDMA)
Near-far Problem	Not Considered (Equal Distance)

Without SIK under the same bandwidth and the same length of spreading code.

In the next section, we evaluate the BER performances of the SS-PPM system.

4. Bit Error Rate Properties [6]-[13]

Here we evaluate the BER performances of the SS-PPM system by computer simulations and a theoretical analysis. Table 3 shows the conditions of the computer simulation and the theoretical analysis.

4. 1 Single Channel BER Properties by Theoretical Analysis [7], [8], [10]-[13]

In the SS-PPM system, the sidelobes of the auto-correlation function appeared in the output of the PN matched filter may be neglected in the theoretical analysis. Therefore, as for the results of the theoretical analysis of the single channel SS-PPM system, the BERs of Without SIK and With SIK are equivalent to those of M-ary orthogonal modulation systems and 2M-ary bi-orthogonal modulation ones, respectively. We will show that these considerations are proper from Figs. 5 and 6 [8], [10]-[12] as shown in later.

BER versus E_b/N_0 for single channel Without SIK (M-ary orthogonal modulation systems) is obtained by substituting Eq. (3) in Eq. (5), and BER versus E_b/N_0 for single channel With SIK (2M-ary bi-orthogonal modulation systems) is obtained by substituting Eq. (4) in Eq. (6); R_{W_1} and R_{W_2} are input signal-to-noise ratios
(SNRs) of the PN matched filter (See Appendix A).

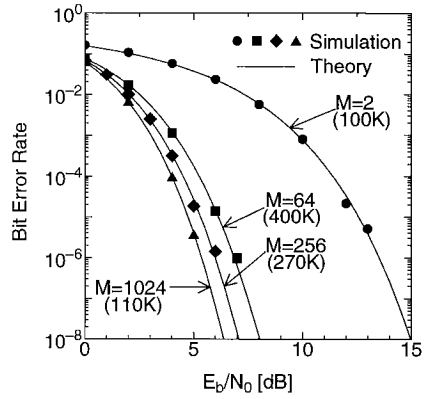

Fig. 5 BERs on single channel Without SIK for various M ($m=1$ [channel], $L=127$ [chip], $R_c=12.7\times10^6$ [cps]).

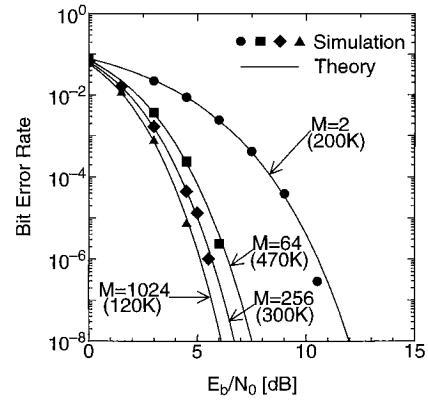

Fig. 6 BERs on single channel With SIK for various M ($m=1$ [channel], $L=127$ [chip], $R_c=12.7\times10^6$ [cps]).

$$R_{W_1}=(\log_2 M)\frac{E_b}{N_0} \tag{3}$$

$$R_{W_2}=(\log_2 2M)\frac{E_b}{N_0} \tag{4}$$

$$P_{W_1}=\frac{M}{2(M-1)}\left(1-\int_{-\infty}^{\infty}\frac{1}{\sqrt{2\pi}}\exp(-z^2/2)\left[\int_{-\infty}^{(z+\sqrt{2R_{W_1}})}\frac{1}{\sqrt{2\pi}}\exp(-x^2/2)\,dx\right]^{M-1}dz\right) \tag{5}$$

$$P_{W_2}=\frac{1}{2}\left(1-\int_{-\infty}^{\infty}\frac{1}{\sqrt{2\pi}}\exp(-z^2/2)\left[1-2\int_{-\infty}^{(-z-\sqrt{2R_{W_2}})}\frac{1}{\sqrt{2\pi}}\exp(-x^2/2)\,dx\right]^{M-1}dz\right) \tag{6}$$

4. 2 Single Channel BER Characteristics [8], [10]-[13]

Figure 5 illustrates the BER versus E_b/N_0 characteristics on the single channel Without SIK for various M, while Fig. 6 shows the BER versus E_b/N_0 characteristics on the single channel With SIK for various M; M means the number of the information slots. In these figures, each solid line shows a theoretical value, and each plot represents a computer simulation's value under the length of spreading code $L=127$ [chip]. These figures illustrate the BER characteristics at $M=$ 2, 64, 256 and 1024 [slot]. In addition, each number put in round brackets shows the data transmissiom rate for each M on condition that the length of spreading code L is 127 [chip] and the chip rate of the spreading code R_c is 12.7×10^6 [cps]; at $M=64$ [slot], for example, the data transmission rates of Without SIK and With SIK are 400 [Kbps] and 470 [Kbps], respectively.

These figures show that each BER characteristic of the computer simulation at $L=127$ [chip] is in good agreement with that of the theory in all the cases of various M, and that each BER characteristic improves with increasing M, and as M increases, it approaches Shannon's limit [8], [10]-[12]. Moreover, we also confirmed that at $L=15$, 31, 63, 255 and 511 [chip], each BER characteristic of the computer simulation is in good agreement with that of the theory in all the cases of various M to the extent of the BER 10^{-6}. Therefore, the agreement indicates that the sidelobes of the auto-correlation function which appeare in the output of the PN matched filter is negligible in the single channel BER characteristics [8], [10]-[12].

Furthermore, in Fig. 7, the BER characteristics on the single channel of the SS-OOK, the SS-DPSK, the SS-BPSK and the SS-PPM systems (Without SIK and With SIK) under the same bandwidth, the same code length and the same data transmission rate are compared. Namely, the chip rate of the spreading code R_c is 12.7×10^6 [cps], and the length of spreading code L is 127 [chip], and the data transmission rate is about 100 [Kbps], and M of Without SIK is 1168 [slot], and M of With SIK is 1317 [slot]. In this figure, each solid line represents the theoretical value for each system.

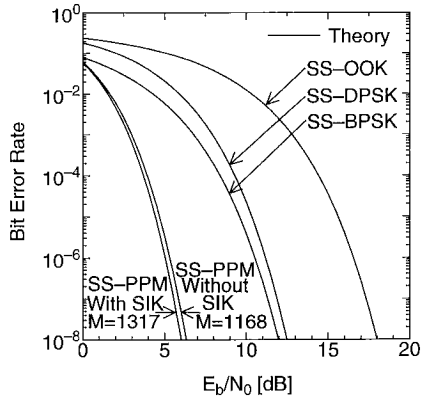

Fig. 7 BERs on single channel SS-OOK, SS-DPSK, SS-BPSK, Without SIK and With SIK under the same bandwidth, the same code length and the same data transmission rate ($m=1$ [channel], $R_c=12.7\times10^6$ [cps], $L=127$ [chip], 100 [Kbps]).

Figure 7 shows that as to E_b/N_0 under the BER 10^{-6}, With SIK is superior about 10 [dB] to the SS-OOK system, 5 [dB] to the SS-DPSK system, 4.5 [dB] to the SS-BPSK system [8], [10]-[13] and 0.4 [dB] to Without SIK [11], [13].

Therefore, on the single channel, Without SIK is superior to the SS-OOK, the SS-BPSK and the SS-DPSK system. Moreover, With SIK is superior to Without SIK.

4. 3 Asynchronous CDMA BER Properties by Theoretical Analysis [9]-[14]

In the asynchronous CDMA of the SS-PPM systems, the effects of the other channel's spreading codes appear in the output of the PN matched filter as cross-correlation functions' values between the PN matched filter's PN code and the other channels' ones. This analysis is carried out on condition that instead of the other channels' interferences, a Gaussian noise whose power is equivalent to the power of the interferences are uniformly added in the SS-PPM's frame; the Gaussian noise is termed a equivalent noise.

Under the above mentioned assumptions, for asynchronous CDMA of Without SIK, BER versus E_b/N_0 is obtained by substituting Eq. (7) in Eq. (5), and for asynchronous CDMA of With SIK, BER versus E_b/N_0 is obtained by substituting Eq. (8) in Eq. (6); R_{W_1} and R_{W_2} are input SNRs of the PN matched filter (See Appendix B). A component corresponded to the other channels' interferences is expressed as the second term of the denominator of Eq. (7) or Eq. (8).

The factor $C_f(M, L)$ in Eq. (7) or Eq. (8) is divided into the following three elements as shown in Eq. (9): 1) The factor of chip asynchronousness is 2/3 (See Appendix C); 2) The factor of cross-correlation characteristic between the spreading codes is F_m (See Appendix D); 3) The factor that the other channels' spreading codes are partially exist in the frame is $B(M, L)$ (See Appendix E).

From Eqs. (5)-(8), it is shown that the parameters determining the CDMA performance of the SS-PPM system are M, m and L.

$$R_{W_1}=\frac{\log_2 M}{\left(\frac{E_b}{N_0}\right)^{-1}+\left(\frac{2(\log_2 M)(m-1)}{M+L-1}\right)C_f(M,L)} \tag{7}$$

$$R_{W_2}=\frac{\log_2 2M}{\left(\frac{E_b}{N_0}\right)^{-1}+\left(\frac{2(\log_2 2M)(m-1)}{M+L-1}\right)C_f(M, L)} \tag{8}$$

$$C_f(M, L)=\frac{2}{3}F_m B(M, L) \tag{9}$$

$$B(M, L)=\frac{1.44(M+L-1)}{L\left\{Q^{-1}\left(\frac{Q(1.2)L}{M+L-1}\right)\right\}^2} \tag{10}$$

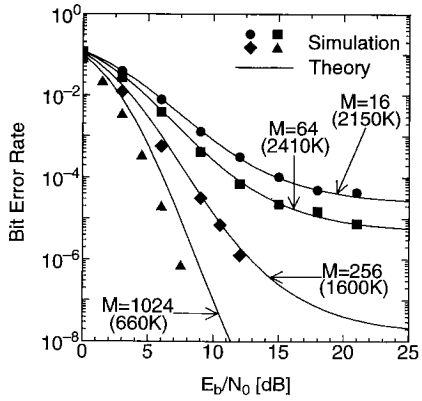

Fig. 8 BERs on asynchronous CDMA of Without SIK for various M (M: parameter, $m=6$ [channel], $L=127$ [chip], $R_c=12.7\times10^6$ [cps]).

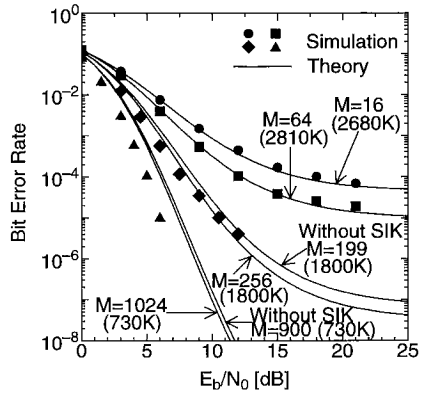

Fig. 9 BERs on asynchronous CDMA of With SIK for various M (M: parameter, $m=6$ [channel], $L=127$ [chip], $R_c=12.7\times10^6$ [cps]).

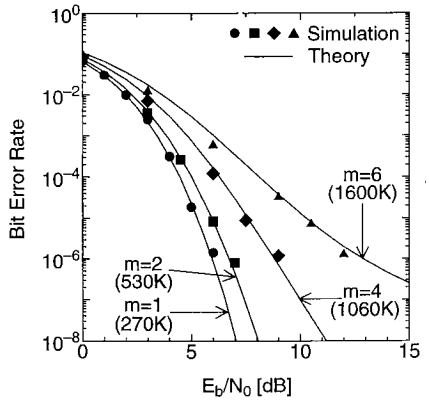

Fig. 10 BERs on asynchronous CDMA of Without SIK for various m ($M=256$ [slot], m: parameter, $L=127$ [chip], $R_c=12.7\times10^6$ [cps]).

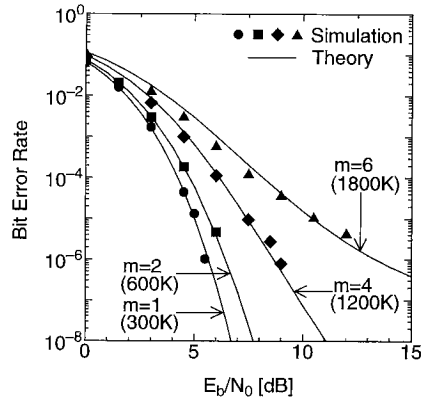

Fig. 11 BERs on asynchronous CDMA of With SIK for various m ($M=256$ [slot], m: parameter, $L=127$ [chip], $R_c=12.7\times10^6$ [cps]).

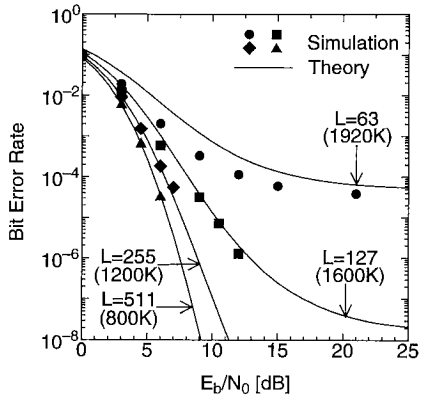

Fig. 12 BERs on asynchronous CDMA of Without SIK for various L ($M=256$ [slot], $m=6$ [channel], L: parameter, $R_c=12.7\times10^6$ [cps]).

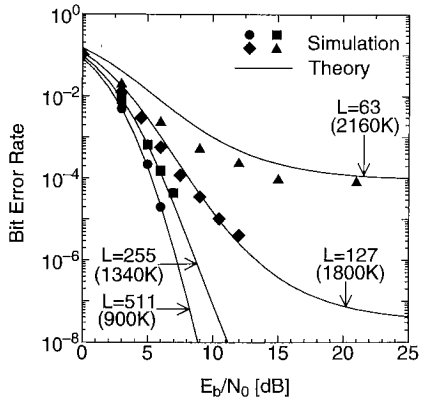

Fig. 13 BERs on asynchronous CDMA of With SIK for various L ($M=256$ [slot], $m=6$ [channel], L: parameter, $R_c=12.7\times10^6$ [cps]).

where, $Q^{-1}(\ )$ is the inverse function of $Q(\ )$ function.

4. 4 Asynchronous CDMA BER Characteristics [8]-[13]

Here, we evaluate the performances of the asynchronous CDMA BER characteristics by the result of the theoretical analysis which we obtain in Sect. 4.3 and computer simulations for various M, m and L; where, M means the number of information slots, and m means the number of multiplex channels, and L means the length of spreading code, as shown in Table 1.

In this section, each figure illustrates BER versus E_b/N_0 characteristic of the SS-PPM system. In Figs. 8-13, each solid line illustrates a theoretical value, and each plot represents a computer simulation's one. In addition, each number puts in round brackets shows the total data transmission rate of all the channels (it is defined as R_T) at $R_c=12.7\times10^6$ [cps]; R_c means the chip rate of the spreading code.

In the following discussions, we evaluate the performance of Without SIK and With SIK.

Firstly, the BER characteristics of Without SIK on condition that M is changed under fixed m and L ($m=6$ [channel], $L=127$ [chip]) are shown in Fig. 8. This figure illustrates the BER characteristics at $M=16$, 64, 256 and 1024 [slot]. At $M=64$ [slot], for example, the total data transmission rate of all the channels R_T is about 2410 [Kbps], because the single channel data transmission rate is about 402 [Kbps] from Eq. (1), and the number of multiplex channels m is 6 [channel]. On the other hand, the BER characteristics of With SIK on condition that M is changed under fixed m and L ($m=6$ [channel], $L=127$ [chip]) are shown in Fig. 9. This figure illustrates the BER characteristics at $M=16$, 64, 256 and 1024[slot]. In addition, under the same m and L, we also illustrate the theoretical values of Without SIK when R_T is 1800 [Kbps] ($M=199$ [slot]), and R_T is 730 [Kbps] ($M=900$ [slot]); these data transmission rates are the same as With SIK's ones when M is 256 [slot], and M is 1024[slot], respectively.

Secondly, the BER characteristics of Without SIK and With SIK on condition that m is changed under M and L fixed ($M=256$ [slot], $L=127$ [chip]) are shown in Figs. 10 and 11, respectively. These figures illustrate the BER characteristics at $m=1$, 2, 4 and 6 [channel].

Finally, the BER characteristics of Without SIK and With SIK on condition that L is changed under M and m fixed ($M=256$ [slot], $m=6$ [channel]) are shown in Figs. 12 and 13, respectively. These figures illustrate the BER characteristics at $L=63$, 127, 255 and 511 [chip].

These figures show that each BER characteristic of the computer simulation is in good agreement with that of the theory [11]-[13], and that the BER characteristic improves with increasing M or L and degrades with increasing m [11]-[13]. Moreover, from Fig. 9, we evaluate the performance of Without SIK and With SIK under the same R_c, the same L and the same R_T; when R_T is 1800 [Kbps], the BER characteristic of With SIK is superior about 1 [dB] to that of Without SIK [13], and when R_T is 730 [Kbps], With SIK is superior about 0.3 [dB] to Without SIK as to E_b/N_0 under the BER 10^{-6} [13].

Thus, it is shown that the asynchronous CDMA BER characteristic of With SIK is better than that of Without SIK under the same total data transmission rate of all the channels R_T, the same bandwidth R_c and the same code length L.

4. 5 Performance Comparison between SS-PPM and the Other Systems

Here, we compare the asynchronous CDMA performances of the SS-PPM system and those of the other conventional SS systems.

Figure 14 illustrates the asynchronous CDMA BER characteristics of With SIK and the usual SS-BPSK system at $L=63$, 127, 255 and 511 [chip]. At each L, R_c and R_T of With SIK are the same as those of SS-BPSK, respectively; namely $R_c=12.7\times10^6$ [cps], and $m=6$ [channel], and the values of M of With SIK are 580 [slot] ($L=63$), 1317 [slot] ($L=127$), 2940 [slot] ($L=255$) and 6500 [slot] ($L=511$); R_T is the total data transmission rate of all the channels. Each solid line shows a theoretical value of With SIK, and each plot connected by a short-dashed line represents a computer simulation's value of the SS-BPSK system, and a longdashed line indicates the theoretical value of the single channel SS-BPSK system. Each number puts in round brackets shows R_T; when $L=63$ [chip], for example, R_T is 1210 [Kbps] in these systems.

This figure shows that as to E_b/N_0 under the BER

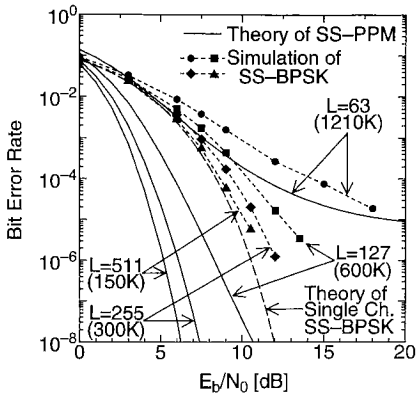

Fig. 14 BERs on asynchronous CDMA of With SIK and usual SS-BPSK under the same bandwidth and the same data transmission rate for various L ($m=6$ [channel], L: parameter, $R_c=12.7\times10^6$ [cps]).

10^{-4}, With SIK is superior about 3.0 [dB] to the SS-BPSK at $L=63$ [chip], about 4.3 [dB] at $L=127$ [chip], about 4.9 [dB]at $L=255$ [chip] and about 4.8 [dB] at $L=511$ [chip]. In the usual SS-BPSK system, as L increases, the asynchronous CDMA BER characteristic approaches the theoretical value of the single channel SS-BPSK system. Similarly, it is considered that in the usual SS-OOK and the usual SS-DPSK system, as L increases, each asynchronous CDMA BER characteristic also approaches each theoretical value of the single channel; however, these system's theoretical values of the single channel are not superior to the SS-BPSK system's one as shown in Fig. 7.

Thus, the asynchronous CDMA BER performance of With SIK is much superior to SS-BPSK, SS-DPSK and SS-OOK under the same bandwidth, the same total data transmission rate and the same code length.

5. Frequency Utilization Efficiency Properties

Here, we evaluate the frequency utilization efficiency η of the SS-PPM system by the result of the theoretical analysis which we obtain in Sect. 4. 3; the frequency utilization efficiency is often used as the performance evaluations of communication systems. Moreover, we compare the frequency utilization efficiency of With SIK and that of the SS-BPSK system.

The frequency utilization efficiencies of Without SIK and With SIK at $M=32$, 64, 128, 256, 512 and 1024 [slot] are illustrated in Figs. 15 and 16, respectively. In these figures, BER is 10^{-3}, and the number of multiplex channels is 6 [channel]. In each M, the value of L varies from 63 to 1023 [chip]. Moreover, in Fig. 16, solid triangles connected by a short-dashed line show the frequency utilization efficiency of the SS-BPSK system calculated by the result of Fig. 14; BER is 10^{-3}, and m is 6 [channel], and the value of L varies from 63 to 1023 [chip].

These figures show that though the asynchronous CDMA is carried out, under the multiplex channels m is 6 [channel] and BER is 10^{-3}, the maximum frequency utilization efficiency η is about 0.22 for Without SIK and about 0.25 for With SIK, respectively. On the other hand, the maximum frequency utilization efficiency of the usual SS-BPSK is about 0.1 under $E_b/N_0=10$ [dB].

Thus, on the frequency utilization efficiency, With SIK is superior to Without SIK, and the SS-PPM system is superior to the SS-BPSK one.

6. Conclusions

As a scheme for increasing the data transmission rate of the binary DS/SS system using only one PN matched filter at the receiver, the SS-PPM system was described; its fundamental structure, the single channel performance, the asynchronous CDMA one and

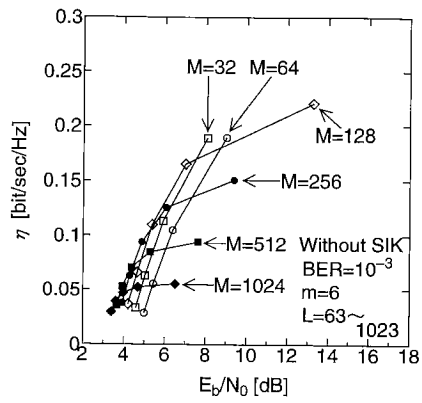

Fig. 15 Frequency utilization efficiency of Without SIK for various M.

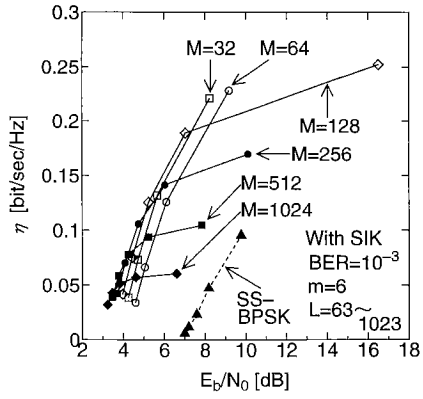

Fig. 16 Frequency utilization efficiency of With SIK for various M.

the frequency utilization efficiency were discussed.

Firstly, we explained the signal structure and the system structure of the SS-PPM system; the SS-PPM system is divided into Without SIK and With SIK.

Secondly, we described the data transmission rate of the SS-PPM system: 1) the SS-PPM system's rate is about 4.0 to 4.8 times higher than the other conventional SS systems' ones; 2) With SIK's rate is about 1.2 times higher than Without SIK's one.

Thirdly, we described the single channel BER characteristic of the SS-PPM system: 1) the BER characteristic improves with increasing M, and as M increases, it approaches Shannon's limit (M is the number of the information slots); 2) under the same bandwidth and the same total data transmission rate, as to E_b/N_0 under the BER 10^{-6}, With SIK is superior about 10 [dB] to the SS-OOK system, 4.5 [dB] to the SS-BPSK system, 5 [dB] to the SS-DPSK system and 0.4 [dB] to Without SIK.

Fourthly, we described the asynchronous CDMA BER characteristic of the SS-PPM system: 1) the BER characteristic improves with increasing M or L and degrades with increasing m(L is the length of the spreading code, and m is the number of multiplex channels); 2) under the same bandwidth, the same

data transmission rate and the same length of spreading code, the BER characteristic of With SIK is superior about 0.3 [dB] to that of Without SIK, and superior about 4 [dB] to that of the SS-BPSK system.

Finally, we described the frequency utilization efficiency of the SS-PPM system: though the asynchronous CDMA is carried out, under the multiplex channel m is 6 [channel] and BER is 10^{-3}, the maximum frequency utilization efficiency η is about 0.22 for Without SIK, and about 0.25 for With SIK, and about 0.10 for the SS-BPSK system, respectively.

Thus the SS-PPM system is superior to the SS-OOK, the SS-BPSK or the SS-DPSK system, and With SIK is superior to Without SIK on the four points: that is, the data transmission rate, the single channel BER, the asynchronous CDMA BER and the frequency utilization efficiency.

Future works are 1) the examinations of the effect of a canceller of cross-correlation components; 2) the implementation of the SS-PPM systems; 3) hardware complexity performance comparisons among SS-PPM, SS-BPSK with FEC, M-ary SS-BPSK using Walsh function and M-ary SS-FSK using Walsh function; 4) the examinations of the frame synchronization and the chip synchronization of the SS-PPM system.

Acknowledgments

The authors would like to thank Prof. M. Haneishi of Saitama University and Prof. M. Nakagawa of Keio University for useful discussions and their great encouragement.

References

[1] Fukui, K., Nanba, A. and Tsubouchi, K., "Baseband Error-Correction Coding for the Asynchronous SS Modem Using a SAW Convolver," *IEICE Technical Report*, SST91-50, Mar. 1992.
[2] Takehara, K., "Spread Spectrum Communication Demodulator Using SAW Devices," *Trans. IEICE*, vol. J74-B-II, no. 5, pp. 262-269, May 1991.
[3] Lindner, J., "The Performance of Code Division Multiplexing with Pulse Position Modulation," *AGARD Conf. Proc.*, no. 239, pp. 35.1-35.11, 1979.
[4] Zhou, X. P., Oka, I. and Fujiwara, C., "Throughput Performance of Time Spread PPM," *IEICE Technical Report*, RCS92-22, Jun. 1992.
[5] Zhou, X. P., Oka, I. and Fujiwara, C., "Bit Error Probability and Throughput Performance of Time Spread PPM/CDMA Systems," *IEICE Trans. Fundamentals*, vol. E75-A, no. 12, pp. 1696-1701, Dec. 1992.
[6] Hasegawa, T. and Hakura, Y., "Spread-Spectrum Pulse Position Modulation —An approach to Shannon limit by simple actual system," *Proc. IEICE Fall Conf. '90*, SB-5-4.
[7] Hasegawa, T., Okazaki, I. and Hakura, Y., "Performance of Spread-Spectrum Pulse Position Modulation," *Proc. IEICE Spring Conf. '91*, B-725.
[8] Okazaki, I. and Hasegawa, T., "A Study on Multiplexing of Spread-Spectrum Pulse Position Modulation," *IEICE Technical Report*, SST91-18, Aug. 1991.
[9] Okazaki, I. and Hasegawa, T., "Performance of Asynchronous Code Division Multiple Access in Spread-Spectrum Pulse Position Modulation," *Proc. of IEICE Spring Conf. '92*, A-207.
[10] Okazaki, I. and Hasegawa, T., "A Study on Derivation of Bit Error Rate of Asynchronous CDMA in SS-PPM System," *IEICE Technical Report*, SST92-8, Apr. 1992.
[11] Okazaki, I. and Hasegawa, T., "On the SS-PPM System and its Asynchronous CDMA," *IEICE Technical Report*, SST92-53, Aug. 1992.
[12] Okazaki, I. and Hasegawa, T., "Spread Spectrum Pulse Position Modulation — A Simple Approach for Shannon's Limit," *Proc. ICCS/ISITA '92*, 12.3, pp. 300-304, Nov. 1992.
[13] Okazaki, I. and Hasegawa, T., "Spread Spectrum Pulse Position Modulation and its Asynchronous CDMA Performance —A Simple Approach for Shannon's Limit," *Proc. ISSSTA '92*, 15-5, pp. 325-328, Nov. 1992.

Appendix A: Input SNRs of PN Matched Filter (Single Channel)

Here, we calculate Eqs. (3) and (4); they are input SNRs of the PN matched filter under the single channel. R_{Wi} means the signal-to-noise ratio (SNR); R_{W_1} is R_{Wi} of Without SIK, and R_{W_2} is R_{Wi} of With SIK. R_{Wi} is given by

$$R_{Wi}=\frac{E_{pi}}{N_0} \tag{A·1}$$

where E_{pi} means the energy of the spreading code per code period, and N_0 means the power spectrum density (PSD) of Gaussian noise.

Moreover, we calculate the value of E_{pi}. Without SIK can transmit $\log_2 M$ bit per spreading code, because Without SIK can transmit $\log_2 M$ bit per frame. Thus, using E_b (it means the energy of the spreading code per bit), E_{pi} of Without SIK (E_{p_1}) is given by Eq. (A·2). On the other hand, using E_b, E_{pi} of Wish SIK (E_{p_2}) is given by Eq. (A·3), because With SIK can transmit $\log_2 2M$ bit per frame.

$$E_{p_1}=(\log_2 M)\,E_b \tag{A·2}$$

$$E_{p_2}=(\log_2 2M)\,E_b \tag{A·3}$$

Therefore, Eq. (3) is obtained by substituting Eq. (A·2) in Eq. (A·1), and Eq. (4) is given by substituting Eq. (A·3) in Eq. (A·1).

Appendix B: Input SNRs of PN Matched Filter (Asynchronous CDMA)

Here, we calculate Eqs. (7) and (8); they mean input SNRs of the PN matched filter under the asynchronous CDMA. R_{W_1} is R_{Wi} of Without SIK, and R_{W_2} is R_{Wi} of With SIK.

On condition that instead of the other channel's interference, a Gaussian noise whose power is equivalent to the power of the interference is uniformly

added in the SS-PPM's frame, N_0 in Eq. (A·1) is assumed to be shown in N_0+N_0'; N_0' means the PSD of the equivalent noise. Thus, R_{Wi} is given by

$$R_{Wi}=\frac{E_{pi}}{N_0+N_0'}=\frac{1}{\frac{N_0}{E_{pi}}+\frac{N_0'}{E_{pi}}} \tag{A·4}$$

where N_0' is obtained by

$$N_0'=(2/R_c)\,\sigma_{pseudo}^2 \tag{A·5}$$

where σ_{pseudo}^2 is the mean square of the equivalent noise, and R_c is the chip rate of the spreading code.

Moreover, we calculate σ_{pseudo}^2 in Eq. (A·5). Figure A·1 shows the mean square of the equivalent noise. In Fig. A·1, $(m-1)$ channels' interferences $(PN_1, PN_2, \cdots, PN_{m-1})$ is added in the SS-PPM system's frame; each mean square of PN_i is defined as σ^2, and its amplitude is defined as A. If only PN_1 is uniformly added in the SS-PPM system's frame, the mean square of the equivalent noise is estimated as $L\sigma^2/(M+L-1)$. Thus, if nearfar problem is not considered, the mean square of the equivalent noise by $(m-1)$ channels' interference is estimated as Eq. (A·6).

$$\sigma_{pseudo}'^2=\frac{(m-1)L\sigma^2}{M+L-1} \tag{A·6}$$

In addition, the mean square of the equivalent noise is multiplied by the factor $C_f(M, L)$; this factor is described in the following appendixes. Thus, σ_{pseudo}^2 is given by

$$\sigma_{pseudo}^2=\frac{(m-1)L\sigma^2}{M+L-1}\,C_f(M, L) \tag{A·7}$$

N_0' is obtained by substituting Eq. (A·7) in Eq. (A·5).

$$N_0'=\frac{2(m-1)L\sigma^2}{(M+L-1)R_c}\,C_f(M, L) \tag{A·8}$$

Since E_{pi} and σ^2 are given by Eqs. (A·9) and (A·10), respectively, N_0'/E_{pi} is obtained by Eq. (A·11).

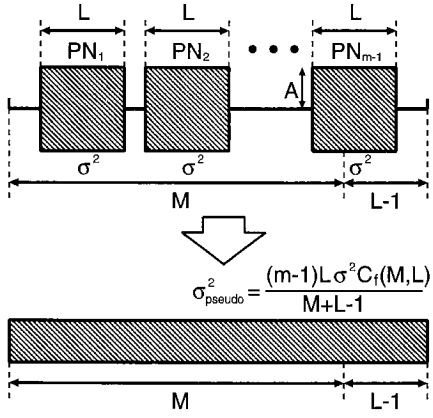

Fig. A·1 Mean square of equivalent noise.

$$E_{pi}=\frac{LA^2}{R_c} \tag{A·9}$$

$$\sigma^2=A^2 \tag{A·10}$$

$$\frac{N_0'}{E_{pi}}=\frac{2(m-1)}{M+L-1}\,C_f(M, L) \tag{A·11}$$

Hence, from Eqs. (A·4) and (A·11), R_{Wi} is given by

$$R_{Wi}=\frac{1}{\frac{N_0}{E_{pi}}+\frac{2(m-1)}{M+L-1}\,C_f(M, L)} \tag{A·12}$$

Therefore, we can obtain Eq. (7) from Eqs. (A·12) and (A·2), and can get Eq. (8) from Eqs. (A·12) and (A·3).

Appendix C: Factor of Chip Asynchronousness; (2/3)

Figure A·2 shows an example of the cross-correlation function appeared in the output of the PN matched filter between the PN matched filter's PN code and the other channels' ones; a solid line shows the cross-correlation function, and closed circles represent the values of the cross-correlation function at the decision-marking instant under the synchronous CDMA, and open circles show the values of the cross-correlation function at the decision-marking instant under the asynchronous CDMA. Each open circle is shifted with α from its neighboring closed circle on the left ($|\alpha|\leqq 1$ [chip]). The value of the mean square of these closed circles is σ_y^2.

We calculate the value of the mean square of these

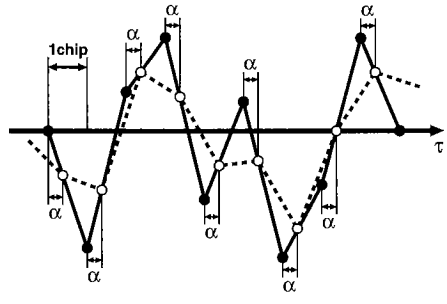

Fig. A·2 Example of cross-correlation function appeared in output of PN matched filter.

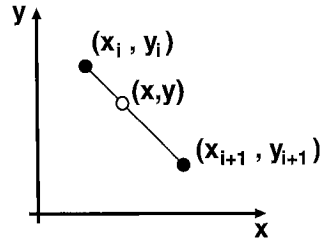

Fig. A·3 Coordinates of cross-correlation function.

open circles; if the coordinates of certain neighboring two closed circles in Fig. A·2 are defined as (x_i, y_i) and (x_{i+1}, y_{i+1}), respectively, the value of the mean square of these open circles corresponds to that of y shown in Fig. A·3. y is obtained by

$$y=\frac{y_{i+1}-y_i}{x_{i+1}-x_i}(x-x_i)+y_i \tag{A·13}$$

where $\overline{y_{i+1}^2}$, $\overline{y_{i+1}y_i}$ and $\overline{y_i^2}$ are given by Eqs. (A·14), (A·15) and (A·16), respectively.

$$\overline{y_{i+1}^2} \rightarrow \sigma_y^2 \tag{A·14}$$

$$\overline{y_{i+1}y_i} \rightarrow 0 \tag{A·15}$$

$$\overline{y_i^2} \rightarrow \sigma_y^2 \tag{A·16}$$

Thus, the mean square of y is given by

$$\overline{\frac{1}{x_{i+1}-x_i}\int_{x_i}^{x_{i+1}} y^2 dx}$$

$$=\frac{1}{3}(\overline{y_{i+1}^2}+\overline{y_{i+1}y_i}+\overline{y_i^2}) \tag{A·17}$$

$$=\frac{2}{3}\sigma_y^2 \tag{A·18}$$

Therefore, as for the value of the mean square of the equivalent noise, the asynchronous CDMA's value is 2/3 times larger than the synchronous CDMA's one.

Appendix D: Factor of Cross-Correlation Characteristic between Spreading Codes; F_m

Though the mean square of the equivalent noise by $(m-1)$ channels' interference at the input of the PN matched filter is estimated as Eq. (A·6), the actual value of the mean square of the equivalent noise is greater than the value of Eq. (A·6) because of the cross-correlation characteristic between the spreading codes as shown in Eq. (A·19); F_m means the factor of the cross-correlation characteristic, and it is larger than 1.

$$\sigma'^2_{pseudo}=F_m\frac{(m-1)L\sigma^2}{M+L-1} \tag{A·19}$$

Table A·1 shows the values of F_m at each L (we confirmed that F_m is independent of m at $m=2$, 4 and 6 [channel]).

Table A·1 Values of the factor of cross-correlation characteristic between spreading codes at each L.

L [chip]	F_m
31	1.23
63	1.10
127	1.03
255	1.00
511	1.00

Appendix E: Factor that the Other Channels' Spreading Codes Are Partially Exist in the Frame; $B(M, L)$

Though the other channels' spreading codes are partially exist in the frame as shown in Fig. A·1, we estimated that these spreading codes are uniformly added in the SS-PPM systems frame as shown in Fig. A·4. Therefore, we considered the factor $B(M, L)$ that the other channels' spreading codes are partially exist in the frame. In Fig. A·4, P_A and P_B represent as the areas of lines drawn at a slant. To obtain $B(M, L)$, we set (A·20) including factor $B(M, L)$.

$$P_AL=P_B(M+L-1) \tag{A·20}$$

where P_A and P_B are given by Eqs. (A·21) and (A·22), respectively.

$$P_A=Q\left(\frac{a\sigma}{\sigma}\right)=Q(a) \tag{A·21}$$

$$P_B=Q\left(\frac{a\sigma}{\sqrt{\frac{B(M, L)L}{M+L-1}}\sigma}\right)$$

$$=Q\left(\sqrt{\frac{a^2(M+L-1)}{B(M, L)L}}\right) \tag{A·22}$$

Equation (A·23) is given by substituting Eqs. (A·21) and (A·22) in Eq. (A·20).

$$Q\left(\sqrt{\frac{a^2(M+L-1)}{B(M, L)L}}\right)=\frac{L}{M+L-1}Q(a) \tag{A·23}$$

Thus, Eq. (A·24) is given by solving Eq. (A·23) for $B(M, L)$.

$$B(M, L)=\frac{a^2(M+L-1)}{L\left\{Q^{-1}\left(\frac{Q(a)L}{M+L-1}\right)\right\}^2} \tag{A·24}$$

We obtained $a=1.2$ from a pre-simulation. Thus, Eq.

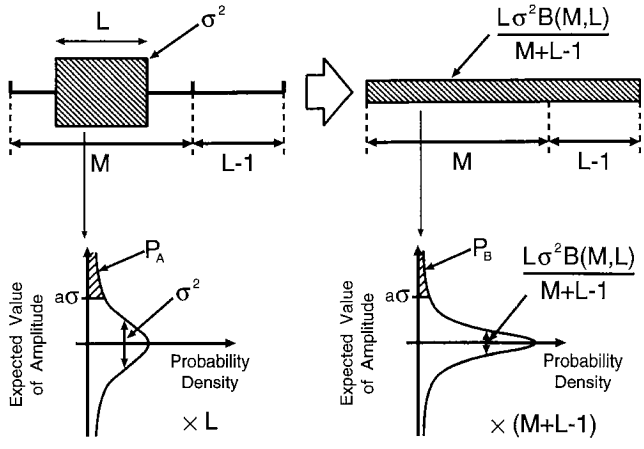

Fig. A·4 Meaning of P_A and P_B.

(A·25) is given by substituting $a=1.2$ in Eq. (A·24).

$$B(M, L)=\frac{1.44(M+L-1)}{L\left\{Q^{-1}\left(\frac{Q(1.2)L}{M+L-1}\right)\right\}^2} \qquad \text{(A·25)}$$

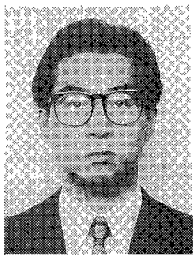

Isao Okazaki was born in Saitama, Japan, on September 8, 1967. He received the B.E. and M.E. degrees in Electrical Engineering from Saitama University, in 1991 and 1993, respectively. Since 1993, he has joined in NTT Radio Communication Systems Laboratories. His research interests are in Spread Spectrum Communications, LAN and Internetworking.

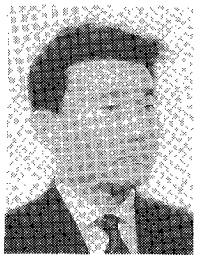

Takaaki Hasegawa was born in Kamakura, Japan, on July 4, 1957. He received the B.E., M.E. and Ph.D. degrees in Electrical Engineering from Keio University, in 1981, 1983 and 1986, respectively. He joined in Faculty of Engineering, Saitama University in 1986. Since 1991 he has been an associate professor. His research interests are in Spread Spectrum Communications, Signal Processing and Human Communications. Dr. Hasegawa is a member of IEEE and SITA of Japan.